



Hydrido iridium(III) complexes of azoaromatic ligands. Isolation, structure and studies of their physicochemical properties

Manashi Panda^a, Nanda D. Paul^a, Sucheta Joy^a, Chen-Hsiung Hung^b, Sreebrata Goswami^{a,*}

^a Department of Inorganic Chemistry, Indian Association for the Cultivation of Science, Jadavpur, Kolkata 700 032, India

^b Department of Chemistry, National Changhua, University of Education, Changhua, Taiwan 500, People's Republic of China

ARTICLE INFO

Article history:

Available online 16 February 2011

Dedicated to Professor S.S. Krishnamurthy.

Keywords:

Azo-aromatics
Hydrido Ir(III) complexes
X-ray crystal structures
Physicochemical properties

ABSTRACT

Reactions of 2-(aryloxy)pyridine (L^{a-c}) with $[\text{IrCl}_3(\text{PPh}_3)_2]$ in two different solvents, viz. ethanol and toluene are reported. In refluxing toluene two new isomeric (*mer* and *fac* geometries) iridium complexes, having molecular formula $[\text{IrCl}_3(\text{PPh}_3)(L)]$ (**1** and **2**) have been isolated. The reaction in refluxing ethanol yielded two new hydrido complexes of molecular formula $[\text{IrHCl}_2(\text{PPh}_3)(L)]$ (**3**) and $[\text{IrHCl}(\text{PPh}_3)_2(L)]\text{Cl}$ (**4**) along with the compound **2**. All the complexes have been thoroughly characterized by NMR, UV–Vis spectroscopy, cyclic voltammetry and X-ray crystallographic analysis. The ^1H NMR spectra of the hydrido complexes **3** and **4** showed a doublet and a triplet signals at $\delta -20.43$ and -14.82 respectively due to coupling with magnetically equivalent phosphorous nuclei. Strong *trans* influence of the π -acceptor ligands guided the X-ray structural parameters; bonds *trans* to the these ligands are unusually long. Similar elongation effect was also noted for the bonds *trans* to the coordinated hydrido ligand. UV–Vis–NIR spectrum consisted of multiple transitions in the UV and visible regions. Cyclic voltammetry of each of these complexes has exhibited a reductive response between -0.25 and -0.55 V, which has been assigned to azo-ligand reduction. The compound **3**, however, showed a quasireversible oxidative wave near 1.45 V, due to $\text{Ir}^{\text{III}}/\text{Ir}^{\text{IV}}$ couple.

© 2011 Elsevier B.V. All rights reserved.

1. Introduction

The chemistry of transition metal hydrido complexes has received increasing attention over the years as the possibilities offered by these compounds for design of homogeneous catalyst as well as preparation of novel complexes [1–10]. The π -acceptor ligands such as carbonyl, mono and polydentate phosphines and cyclopentadienyl groups play significant roles [10–14] in stabilization of such complexes. Literature survey has however revealed that the corresponding complexes containing N-donor ligands [15–25] have been less attended. The influence of the ancillary ligand on the reactivity of M–H bond is of interest and the role of N-donor ligands in this context is now emerging [25–28].

We have a long standing interest in the coordination chemistry of transition metal complexes of the π -acceptor azoaromatic ligands [29–36]. The platinum group metal complexes of 2-(aryloxy)pyridine (abbreviated as L, Chart 1) ligand system have been the subject of considerable interest because of their rich redox, spectroscopic behavior, catalytic activities and isomerization reactions [37–40,4–8,10]. Iridium complexes in general and the corresponding hydrido complexes, in particular, are effective in the

context of their activities as homogeneous catalysts [1–10] and biological activities [41–44]. It may be worth noting here that we recently have reported two novel mixed ligand chloro complexes of L [32]. The first one is a chloro bischelated complex of iridium where one of the two coordinated ligands (L) binds as an anionic C, N-donor revealing a new coordination mode of L, while the other one is a rare mixed ligand iridium(V) complex. In this work two strong π accepting ligands viz. L and triphenyl phosphine are used to stabilize Ir–H complexes. This report discloses the results of the reaction between $[\text{IrCl}_3(\text{PPh}_3)_2]$ [45] and the ligand L. The hydrido complexes were successfully isolated from alcoholic reaction medium (Scheme 1).

2. Results and discussion

2.1. Synthesis and characterization

The three ligands, viz. L^a , L^b and L^c differing with respect to substitution on the phenyl ring are used in this work. The ligands and the isolated compounds are collected in Chart 1.

Reaction of $[\text{IrCl}_3(\text{PPh}_3)_2]$ and the ligand L in equimolar proportion in toluene produced a brown solution which on chromatographic purification and subsequent crystallization yielded two pure compounds **1** and **2** of identical molecular formulae

* Corresponding author. Tel.: +91 3324734971; fax: +91 3324732805.

E-mail address: icsg@iacs.res.in (S. Goswami).

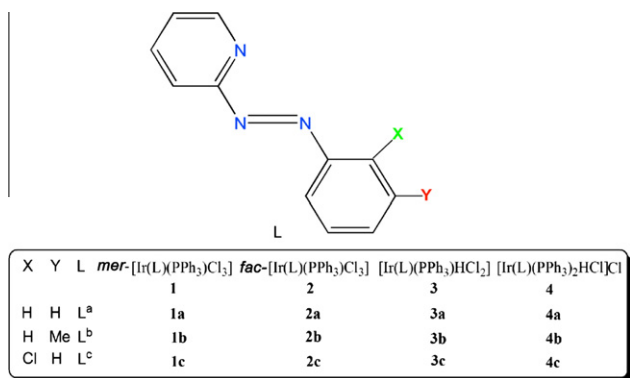


Chart 1. Ligands and corresponding iridium complexes.

[IrCl₃(PPh₃)(L)] in 45% and 25% yield respectively (Scheme 1). These compounds are geometrical isomers (*vide infra*). The color of the compound **1** is brown while that of the compound **2** is greenish yellow.

In an identical reaction of [IrCl₃(PPh₃)₂] with L in 1:1 molar ratio in boiling ethanol produced a greenish brown solution which on subsequent purification produced two new hydrido complexes of molecular formula [IrHCl₂(PPh₃)(L)] (**3**) and [IrHCl(PPh₃)₂(L)]Cl (**4**) along with the compound **2** as a minor product (yield: 8–10%) (Scheme 1). An identical set of products were also obtained when the reactions were carried out in toluene containing only a few drops of ethanol. It is not surprising since alcoholic solvents have commonly been used for the synthesis of metal–hydrido complexes [46,47].

These complexes, **1–4** gave satisfactory elemental analyses (*cf.*, Experimental). Electrospray mass spectra of the complexes corroborate with their formulations as described above. For example, the complexes **1a**, **2b**, **3b** and **4b** showed intense peaks due to the molecular ion [**1a** + Na]⁺, [**2b** + Na]⁺, [**3b** + Na]⁺ and [**4b** – Cl]⁺ at *m/z*, 766, 780, 746 and 950 amu, respectively. Notably, the experimental spectral features of the complexes correspond very well to the simulated isotopic pattern for the given formulations. Representative spectra of all the complexes along with the simulated spectra are submitted as Supporting Information, Figs. S1–4.

The complexes possess *S* = 0 ground state, as determined by magnetic susceptibility measurements at room temperature. These showed resolved ¹H NMR spectra in CDCl₃: strong intensity peaks were observed in the region δ 7.99–7.90 and 7.44–7.32 due to the presence of coordinated PPh₃ ligand [48–49]. Some resonances originated from the coordinated L overlapped with that of PPh₃. The peaks in the range δ 8.82–7.47 and 7.84–7.06 are assigned to pyridyl and phenyl resonances, respectively. The most notable observation in the spectrum of **3** is the appearance of a distinct doublet at δ –20.43, which confirms the presence of coordinated

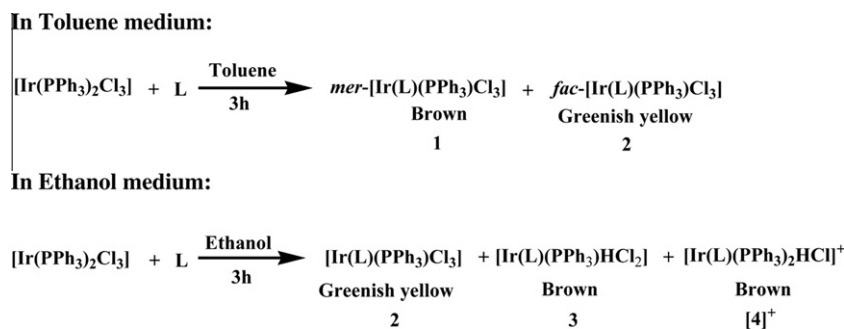
hydride. The coupling between hydrogen and phosphorous nucleus generates this doublet pattern. In the complex **4** hydride resonance appeared at δ –14.82 as a triplet due to coupling with two magnetically equivalent phosphorous nuclei [50,51]. The ¹H NMR spectra of all the complexes are submitted as the Supporting Information (Figs. S5–8).

2.2. Crystal structure

Suitable crystals for X-ray structure determination of **1c**, **2c**, **3a** and **4c** were obtained by slow diffusion of dichloromethane solutions of the compounds into hexane. Oak Ridge thermal-ellipsoid plot (ORTEP) and atom numbering schemes of the above complexes are shown in Figs. 1–4, crystallographic parameters and selected bond lengths are collected in Tables 1 and 2 respectively.

Structural analysis of **1c** and **2c** indeed confirmed their isomeric nature. In both these complexes the central Ir-center is hexa-coordinated and surrounded by three chlorides, a triphenylphosphine and a bidentate azoaromatic ligand, L^c producing a distorted octahedral environment. The complex **1c** is meridional (*mer*) with respect to the three coordinated Cl atoms while **2c** is facial (*fac*). In **1c** two chlorides are disposed *trans* occupying two axial positions, while the PPh₃ is *trans* to azo-N and one of the chlorides is *trans* to the pyridyl-N. Simplified drawings of coordinated atoms in the two reference complexes are shown in Chart 2 for comparison. The equatorial plane of **2c** is formed by the two mutually *cis* disposed chlorine atoms, Cl(1)–Ir(1)–Cl(3), 89.06(6)° and the two chelating nitrogen atoms of the diazo ligand with the bite angle, N(3)–Ir(1)–N(1), 77.4(2)°, which is considerably lower than the ideal value for an octahedral geometry. The Ir–Cl lengths are significantly affected by different *trans* influences [52–54] of the pyridyl-N/azo-N and PPh₃ ligands. For example, the Ir(1)–Cl(2) bond length in **2c** is *trans* to PPh₃ and is consequently unusually long. The azo bonds are within the normal range of coordinated azo ligands [29–35,55].

The X-ray structure of **3a** is similar to that of the [IrCl₃(PPh₃)(L^c)] (**1c**), except that a hydride is coordinated to iridium *trans* to pyridyl-N instead of a chloride ligand. The ligand L^a binds iridium using N(1) and N(3) atoms and the chelate bite angle is N(1)–Ir(1)–N(3), 74.83(7)°. Two chloride ligands occupy the *trans* axial positions (Cl(1)–Ir(1)–Cl(2), 173.046(18)°). In the equatorial plane, the PPh₃ ligand and azo-N are nearly *trans* disposed with the angle P(1)–Ir(1)–N(1), 177.43(4)° and the pyridyl-N is *trans* to the hydride (H(102)–Ir(1)–N(3), 173.0(8)°). The bulky PPh₃ group displaced away from the L^a ligand towards the smaller hydride ligand. Notably the Ir–N(pyridine) distance is longer than that observed in **1c** and **2c** (*av.* 2.069 Å), but is similar to that (*av.* 2.150(5) Å) in [IrH₂(PPh₃)₂(bpy)]. The strong *trans* influence [52–54] of hydride is expected to cause lengthening of the *trans* Ir–N bonds.



Scheme 1. Syntheses of the complexes.

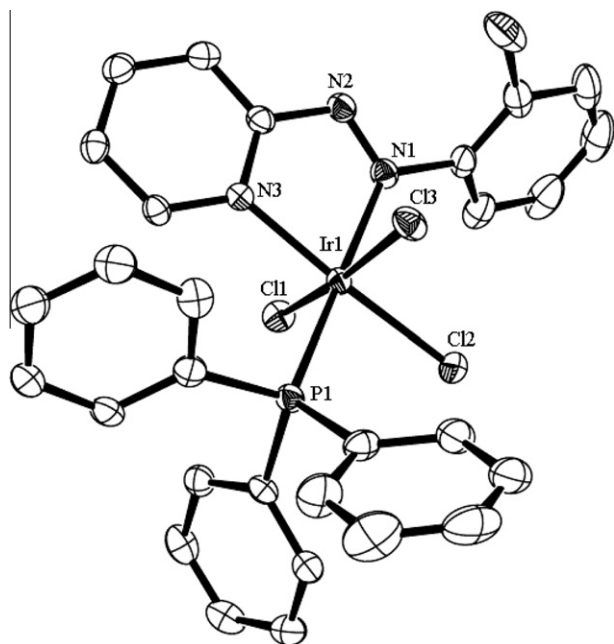


Fig. 1. An ORTEP and atom numbering scheme for *mer*-[IrCl₃(PPh₃)(L⁵)](**1c**). Hydrogen atoms are not shown for clarity. Thermal ellipsoids are shown in 30% probability.

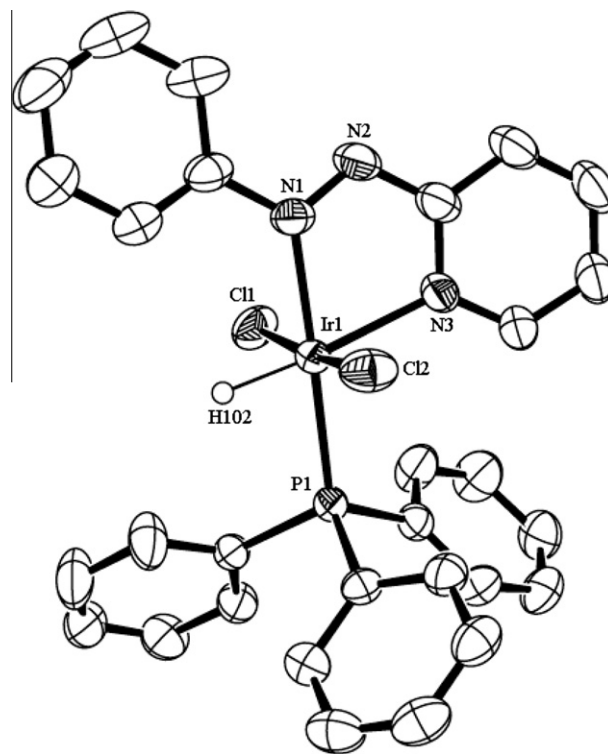


Fig. 3. An ORTEP and atom numbering scheme for [IrHCl₂(PPh₃)(L⁵)](**3a**). Hydrogen atoms are not shown for clarity. Thermal ellipsoids are shown in 30% probability.

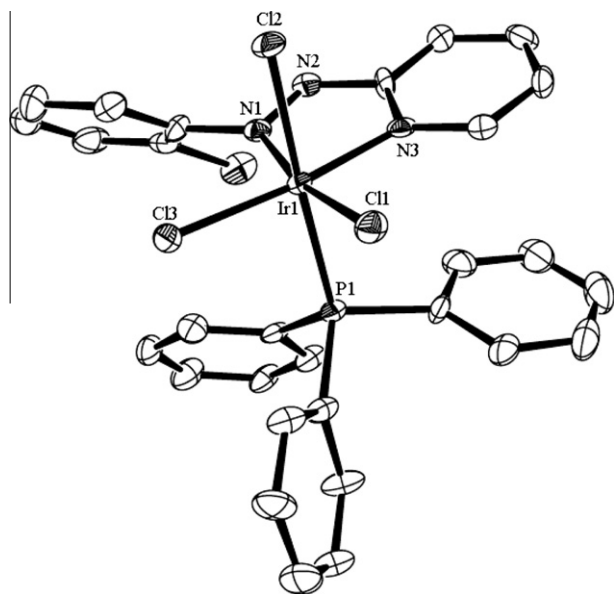


Fig. 2. An ORTEP and atom numbering scheme for *fac*-[IrCl₃(PPh₃)(L⁵)](**2c**). Hydrogen atoms are not shown for clarity. Thermal ellipsoids are shown in 30% probability.

The structure of the cationic part of the compound **4c** consists of a nearly planar Ir₂HCl moiety with a bent P(1)–Ir(1)–P(2) (166.10(6)°) grouping perpendicular to this plane. The bidentate ligand L⁵ chelates the iridium ion through N(1) and N(3) with a bite angle N(1)–Ir(1)–N(3), 76.0(2)°. The octahedral coordination, typical of the Ir(III) complexes, is appreciably distorted because of chelation and very different bulkiness of the ligands. As a consequence of smallest occupancy of the hydride ligand, the two *trans* PPh₃ groups bent towards hydride to minimize the steric repulsion resulting the P(1)–Ir(1)–P(2) angle much smaller than 180°. The Ir(1)–N(pyridine) length (2.125(5) Å), which is *trans* to the hydride

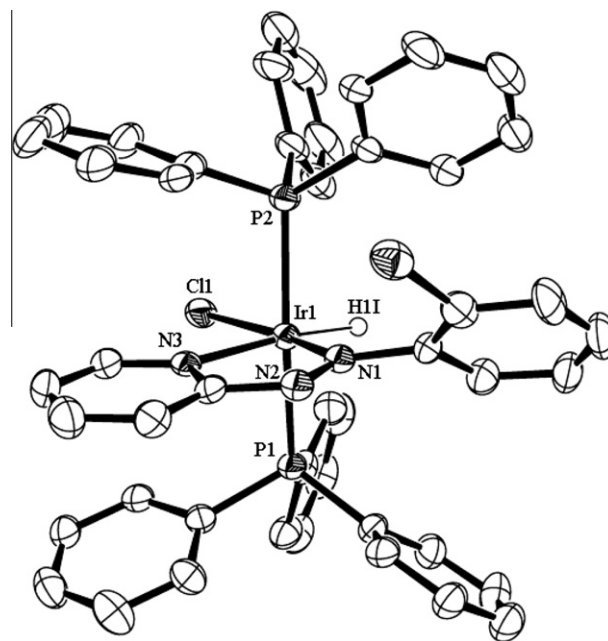


Fig. 4. An ORTEP and atom numbering scheme for the cationic part of [IrHCl(PPh₃)₂(L⁵)]Cl(**4c**). Hydrogen atoms are not shown for clarity. Thermal ellipsoids are shown in 30% probability.

ligand, is elongated considerably as expected [52–54]. Rest of the structural parameters are in the normal range.

2.3. Electronic spectra

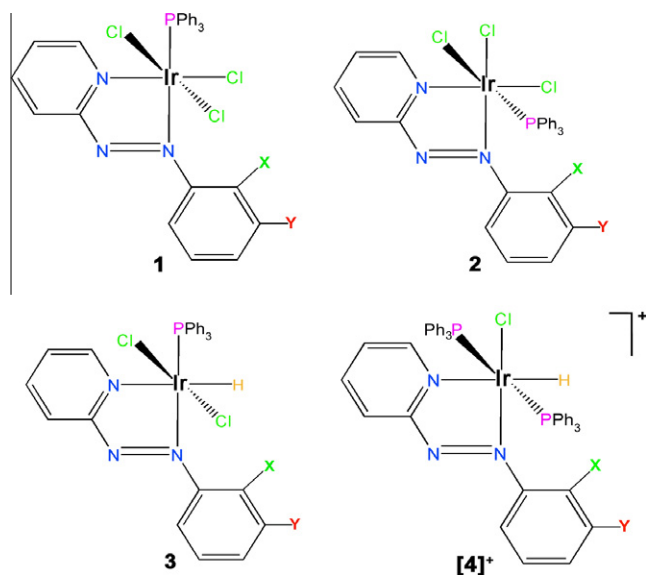
All the compounds **1–4** are freely soluble in non-polar solvents like dichloromethane, chloroform and their electronic spectra

Table 1
Crystallographic Data of **1c**, **2c**, **3a** and **4c**.

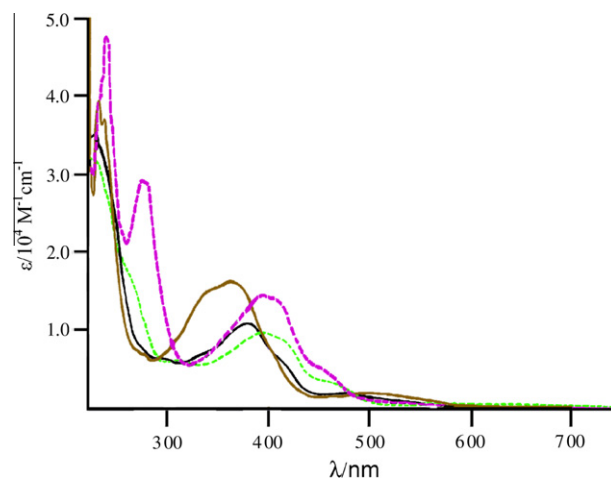
	1c	2c	3a	4c
Empirical formula	C ₂₉ H ₂₃ Cl ₄ IrN ₃ P	C ₂₉ H ₂₃ Cl ₄ IrN ₃ P ₂ O	C ₂₉ H ₂₅ Cl ₂ IrN ₃ P	C ₄₇ H ₃₉ Cl ₂ IrN ₃ P ₂ , 0.5(Cl), 0.5(Cl)
Molecular mass	778.49	794.49	709.61	1006.32
Temperature (K)	150	173	293	150
Crystal system	Monoclinic	Trigonal	Monoclinic	Monoclinic
Space group	P21/c	P31	P21/n	C2/c
<i>a</i> (Å)	11.4928(2)	9.8210(1)	17.6463(10)	32.9255(10)
<i>b</i> (Å)	15.1937(3)	9.8210(1)	9.3033(5)	15.0264(4)
<i>c</i> (Å)	16.7995(3)	26.3302(7)	18.1635(10)	23.4681(7)
α (°)	90	90	90	90
β (°)	100.099(1)	90	114.221(1)	129.948(2)
γ (°)	90	120	90	90
<i>V</i> (Å ³)	2888.05(9)	2199.36(7)	2719.4(3)	8901.2(5)
<i>Z</i>	4	3	4	8
<i>D</i> _{calc.} (g/cm ³)	1.791	1.800	1.733	1.502
Cryst. dimens. (mm)	0.18 × 0.10 × 0.08	0.20 × 0.12 × 0.08	0.22 × 0.14 × 0.08	0.10 × 0.04 × 0.03
θ Range for data coll (°)	1.8, 30.0	2.3, 30.0	2.1, 30.1	1.6, 30.0
Goodness-of-fit (GOF)	1.00	0.99	0.79	1.02
Reflns. collected	31292	22989	33928	57261
Unique reflns.	8436	8268	7986	12992
Largest diff. between peak and hole (e Å ⁻³)	-0.83, 0.63	-2.38, 3.46	-1.15, 0.73	-2.34, 6.56
Final <i>R</i> indices [<i>I</i> > 2 σ (<i>I</i>)]	<i>R</i> ₁ = 0.0231 <i>wR</i> ₂ = 0.0490	<i>R</i> ₁ = 0.0419 <i>wR</i> ₂ = 0.0879	<i>R</i> ₁ = 0.0191 <i>wR</i> ₂ = 0.0521	<i>R</i> ₁ = 0.0566 <i>wR</i> ₂ = 0.1739

Table 2
Selected Bond Lengths of **1c**, **2c**, **3a** and **4c**.

Bond	1c	2c	3a	4c
Ir1–N1	2.084(2)	2.011(5)	2.098(18)	2.003(5)
Ir1–N3	2.051(18)	2.003(6)	2.160(19)	2.125(5)
Ir1–P1	2.325(6)	2.316(16)	2.273(5)	2.365(16)
Ir1–Cl1	2.360(6)	2.340(17)	2.362(6)	2.372(14)
Ir1–Cl2/P2 ^a	2.359(6)	2.403(15)	2.341(6)	2.338(17)
Ir1–Cl3/H ^b	2.357(6)	2.356(17)	1.490(2)	1.600(11)
N2–N1	1.263(3)	1.305(7)	1.262(3)	1.281(7)

^a For **4c**.^b For **3a** and **4c**.**Chart 2.** Geometries of the complexes **1**, **2**, **3** and **4**.

were recorded in dichloromethane solution. The compounds [IrCl₃(PPh₃)(L)], **1** showed an intense absorption near 380 nm (ϵ , ca. 10775 M⁻¹ cm⁻¹) and two shoulders at 415 nm (ϵ , ca. 6085 M⁻¹ cm⁻¹) and 363 nm (ϵ , ca. 9610 M⁻¹ cm⁻¹) followed

**Fig. 5.** Electronic spectra of **1a** (black), **2a** (green), **3a** (brown) and **4a** (violet). (For interpretation of the references to color in this figure legend, the reader is referred to the web version of this article.)

by two weak transitions at 485 nm (ϵ , ca. 1885 M⁻¹ cm⁻¹) and 560 nm (ϵ , ca. 800 M⁻¹ cm⁻¹), the isomeric compounds [IrCl₃(PPh₃)(L)], **2** on the other hand showed a broad transition at around 400 nm (ϵ , ca. 8500 M⁻¹ cm⁻¹) along with two weak transitions near 460 nm (ϵ , ca. 3570 M⁻¹ cm⁻¹) and 630 nm (ϵ , ca. 500 M⁻¹ cm⁻¹). The hydrido complexes [IrHCl₂(PPh₃)(L)], **3** exhibited an intense and broad transition at 360 nm (ϵ , ca. 15975 M⁻¹ cm⁻¹), two shoulders at 400 and 336 nm along with a weak transition at long wavelength region, 515 nm (ϵ , ca. 2190 M⁻¹ cm⁻¹). The compounds [IrHCl(PPh₃)₂(L)]Cl, **4** showed a broad transition near 400 nm (ϵ , ca. 13795 M⁻¹ cm⁻¹) along with two weak transitions at 460 nm (ϵ , ca. 4985) and 565 nm (ϵ , ca. 780 M⁻¹ cm⁻¹). Representative UV–Vis spectra are displayed in Fig. 5 and spectral data are collected in Table 3.

The transitions of high intensities at the lower energy part of the spectra are presumably due to metal to ligand charge transfer (MLCT) [48,49]. The weaker absorption tails exhibited by the iridium complexes, **2** and **4**, in the lower energy region may be ascribed to forbidden ³MLCT ($d\pi(\text{Ir})-\pi^*(\text{ligand})$) transitions [56].

Table 3
Electronic spectral data.

Compound	Electronic Spectra ^a [$\lambda_{\text{max}}/\text{nm}$ ($\epsilon/\text{M}^{-1}\text{cm}^{-1}$)]
[IrCl ₃ (PPh ₃)(L ^{1a})](1a)	560(800), 485(1885), 413(6085) ^b , 380(10775), 363(9610) ^b , 297(6270), 228(32855)
[IrCl ₃ (PPh ₃)(L ^{1b})](1b)	558(825), 485(2045), 422(6830) ^b , 384(10060), 297(6280), 230(35210)
[IrCl ₃ (PPh ₃)(L ^{1c})](1c)	564(785), 485(2010), 425(6575) ^b , 383(10585), 365(6945) ^b , 298(7080), 230(33970)
[IrCl ₃ (PPh ₃)(L ^{1a})](2a)	632(470), 462(3570) ^b , 417(8540) ^b , 393(9530), 312(5925), 230(30740)
[IrCl ₃ (PPh ₃)(L ^{1b})](2b)	630(495), 465(3700) ^b , 405(9350), 310(5235), 228(31690)
[IrCl ₃ (PPh ₃)(L ^{1c})](2c)	633(466), 460(3305) ^b , 370(7515), 310(5840), 228(29460)
[IrHCl ₂ (PPh ₃)(L ^{1a})](3a)	515(2190), 400(7800) ^b , 362(15975), 336(14715) ^b , 228(39070)
[IrHCl ₂ (PPh ₃)(L ^{1b})](3b)	511(2065), 406(8120) ^b , 367(14210), 334(12135) ^b , 230(35250)
[IrHCl ₂ (PPh ₃)(L ^{1c})](3c)	503(1905), 329(10355), 228(38510)
[IrHCl(PPh ₃) ₂ (L ^{1a})]Cl(4a)	565(780), 456(4985) ^b , 408(13795) ^b , 391(14370), 273(28555), 235(45260)
[IrHCl(PPh ₃) ₂ (L ^{1b})]Cl(4b)	565(875), 457(5775) ^b , 403(13285), 273(26305), 236(42230)
[IrHCl(PPh ₃) ₂ (L ^{1c})]Cl(4c)	564(890), 460(4080) ^b , 395(10695), 273(24690), 235(41485)

^a In dichloromethane.^b Shoulder**Table 4**
Electrochemical data^a.

Compound	Oxidation $E_{1/2}^b/\text{V}$ ($\Delta E_p/\text{mV}$)	Reduction $-E_{1/2}^b/\text{V}$ ($\Delta E_p/\text{mV}$)
[IrCl ₃ (PPh ₃)(L ^{1a})](1a)		0.41(110)
[IrCl ₃ (PPh ₃)(L ^{1b})](1b)		0.42(90)
[IrCl ₃ (PPh ₃)(L ^{1c})](1c)		0.36(100)
[IrCl ₃ (PPh ₃)(L ^{1a})](2a)		0.32(90)
[IrCl ₃ (PPh ₃)(L ^{1b})](2b)		0.34(90)
[IrCl ₃ (PPh ₃)(L ^{1c})](2c)		0.30(110)
[IrHCl ₂ (PPh ₃)(L ^{1a})](3a)	1.45 ^c	0.55(100)
[IrHCl ₂ (PPh ₃)(L ^{1b})](3b)	1.48 ^c	0.58(120)
[IrHCl ₂ (PPh ₃)(L ^{1c})](3c)	1.55 ^c	0.50(120)
[IrHCl(PPh ₃) ₂ (L ^{1a})]Cl(4a)		0.27(90)
[IrHCl(PPh ₃) ₂ (L ^{1b})]Cl(4b)		0.32(90)
[IrHCl(PPh ₃) ₂ (L ^{1c})]Cl(4c)		0.24(100)

^a Conditions: solvent, dichloromethane; supporting electrolyte, NBu₄ClO₄ (0.1 M); working electrode, platinum for oxidation and reduction processes; reference electrode, SCE; solute concentration, ca. 10⁻³(M); scan rate, 50 mV s⁻¹.^b $E_{1/2} = \frac{1}{2}(E_{\text{pa}} + E_{\text{pc}})$, $\Delta E_p = E_{\text{pa}} - E_{\text{pc}}$ in mV (E_{pa} = anodic peak potential, E_{pc} = cathodic peak potential).^c Irreversible value corresponds to E_{pa} .

The strong transitions in the UV region (<350 nm) are attributable to intra-ligand charge transfer transitions [29–35].

2.4. Redox properties

The redox behavior of all the reference complexes was studied by cyclic voltammetry in dichloromethane (0.1 M TBAP), in the potential range +1.5 to –1.5 V, using a platinum working electrode. The potentials are referenced to the saturated calomel electrode (SCE) and the data are collected in Table 4. Segmented voltammograms (cathodic sweep) of the representative compounds are displayed in Fig. 6.

Nature of the voltammograms of the compounds *mer*-[IrCl₃(PPh₃)(L)], **1** and *fac*-[IrCl₃(PPh₃)(L)], **2** is similar. An electrochemically reversible cathodic response near –0.4 V was observed for the compound **1** and that for **2** was observed near –0.3 V. This shift of potential indicates that the acceptor level (LUMO) in the

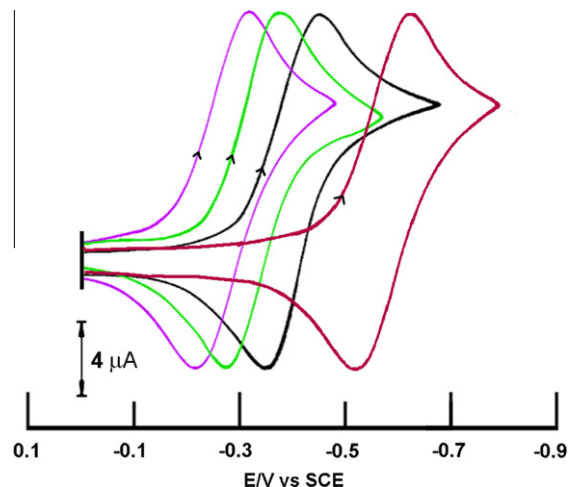


Fig. 6. Segmented cyclic voltammograms of **1a** (black), **2a** (green), **3a** (brown) and **4a** (violet). (For interpretation of the references to color in this figure legend, the reader is referred to the web version of this article.)

fac-isomer is more accessible to reduction than the corresponding *mer*-isomer. On the other hand, voltammograms of the hydrido complexes, [IrHCl₂(PPh₃)(L)], **3** and [IrHCl(PPh₃)₂(L)]Cl, **4** also consisted of a reversible cathodic response but have a significant difference in E^0 values. While the compound **4** exhibited a reductive wave at –0.27 V, the response in the compound **3** moved cathodic to –0.55 V indicating that the cationic compound **4** is more easily reduced than the neutral compound **3**. The one-electron redox response has been confirmed by constant-potential electrolysis for all the reversible waves. The redox potentials are found to be sensitive to the nature of substitution on the phenyl ring. Thus, a systematic anodic shift of the redox potentials was observed upon moving from electron donating –Me substituted ligand (L^b) complex to the electron withdrawing Cl ligand (L^b) complex (Table 3). It may be noted here that the free ligand L is known to undergo two-step reductions at –1.31 and –1.57 V [29–35]. The response in the cathodic potentials for the above complexes are ascribed to the reduction of L ligand. In all the complexes, reported herein, the potential of the reduction process is shifted toward at more positive value because of the strong electronic pull of the metal ion (Ir^{III}). After coordination the azo ligand becomes electron deficient and hence is more easily reduced than the free (uncoordinated) ligand. Similar trend has been noted before in the several reported compounds of L. However, we failed to observe the second reduction process of the coordinated azo-function which possibly falls outside the accessible voltage window. In addition, the compound **3** also showed an irreversible oxidative wave with no cathodic counterpart at 1.45 V. Comparing with previously reported Ir–L complexes [32] this is assigned to a Ir^{III}/Ir^{IV} process.

3. Conclusion

Two novel mixed ligand Ir(III) hydrido complexes have been synthesized using two strong π -acidic ligands, viz. 2-(aryloxy)pyridine and PPh₃ in EtOH. Non-alcoholic solvent, toluene failed to produce the hydrido complexes and two new isomeric non-hydrido complexes were obtained. Alcoholic solvents play the pivotal role in Ir–H bond formation. These complexes constitute new examples of Iridium complexes with strong π accepting N-donor ligands where the ligand L stabilizes the iridium(III) state preferably. All the complexes show rich physicochemical properties. Hydride complexes with N-donor ligands are important in the field of reactivity studies of Ir–H bonds. Our work in this area is ongoing.

4. Experimental

4.1. Materials

$\text{IrCl}_3 \cdot x\text{H}_2\text{O}$ was obtained from Arora Matthey and was digested twice with concentrated HCl before use. Solvents and chemicals used for syntheses were of analytical grade and used as received. Supporting electrolyte (TEAP) [57] and solvents for electrochemical work were obtained as before. 2-(Arylazo)pyridines were prepared following the reported procedure [58]. *Caution! Perchlorate salts have to be handled with care and with appropriate safety precautions.*

4.2. Methods

UV–VIS–NIR absorption spectrum was recorded on a Perkin–Elmer Lambda 950 UV/VIS spectrophotometer. NMR spectra were taken on a Bruker Avance DPX 300 spectrometer. Infrared spectra were obtained using a Perkin–Elmer 783 spectrophotometer. Cyclic voltammetry was carried out in 0.1 M Bu_4NClO_4 solutions using a three-electrode configuration and a PC-controlled PAR model 273A electrochemistry system. The $E_{1/2}$ for the ferrocenium–ferrocene couple under our experimental condition was 0.39 V. A Perkin–Elmer 240C elemental analyzer was used to collect micro analytical data (C, H, N).

4.3. Syntheses

4.3.1. Reaction of $[\text{IrCl}_3(\text{PPh}_3)_2]$ with 2-(arylazo)pyridine (L^{a-c}) in toluene

4.3.1.1. Isolation of $[\text{IrCl}_3(\text{PPh}_3)(L^a)]$ (1a**), $[\text{IrCl}_3(\text{PPh}_3)(L^a)]$ (**2a**).** The reaction mixture of $[\text{IrCl}_3(\text{PPh}_3)_2]$ and the ligand L^a in equimolar proportion was heated at reflux in toluene for 3 h. During this period, initial orange color of the mixture became brown. Two pure compounds **1** and **2** of identical molecular formulae $[\text{IrCl}_3(\text{PPh}_3)(L^a)]$ were isolated from the crude mass.

The pure compounds were isolated from the crude mixture on preparative TLC (Thin Layer Chromatography) silica-gel plate. It was first eluted with toluene–chloroform (1:9) solvent mixture. The compound **1** moved first as the top brown band and was isolated. Another band, greenish yellow in color, was then separated out on elution with chloroform–acetonitrile (4:1) solvent mixture. The compound **2** was obtained by the evaporation of the above eluate. The yields and characterization data of **1a** and **2a** are as follows.

$[\text{IrCl}_3(\text{PPh}_3)(L^a)]$ (**1a**). Yield: 45%, FT-IR (KBr, cm^{-1}): 1615 $[\nu(\text{C}=\text{N})]$, 1405 $[\nu(\text{N}=\text{N})]$, 530, 695 and 745 $[\nu(\text{PPh}_3)]$, ESI-MS, m/z : 766 $[\text{M}+\text{Na}]^+$. Anal. Calc. for $\text{C}_{29}\text{H}_{24}\text{N}_3\text{Cl}_3\text{P}_3\text{Ir}$: C, 46.82; H, 3.25; N, 5.65. Found: C, 46.85; H, 3.22; N, 5.64.

$[\text{IrCl}_3(\text{PPh}_3)(L^a)]$ (**2a**). Yield: 25%, FT-IR (KBr, cm^{-1}): 1595 $[\nu(\text{C}=\text{N})]$, 1380 $[\nu(\text{N}=\text{N})]$, 530, 595 and 750 cm^{-1} $[\nu(\text{PPh}_3)]$, ESI-MS, m/z : 766 $[\text{M}+\text{Na}]^+$. Anal. Calc. for $\text{C}_{29}\text{H}_{24}\text{N}_3\text{Cl}_3\text{P}_3\text{Ir}$: C, 46.82; H, 3.25; N, 5.65. Found: C, 46.79; H, 3.27; N, 5.62.

Other substituted complexes (**1b**, **2b** and **1c**, **2c**) were similarly synthesized using the L^b and L^c ligands in place of L^a . Their yields and characterization data are as follows.

$[\text{IrCl}_3(\text{PPh}_3)(L^b)]$ (**1b**). Yield: 45%, FT-IR (KBr, cm^{-1}): 1615 $[\nu(\text{C}=\text{N})]$, 1405 $[\nu(\text{N}=\text{N})]$, 530, 695 and 745 $[\nu(\text{PPh}_3)]$, ESI-MS, m/z : 780 $[\text{M}+\text{Na}]^+$. Anal. Calc. for $\text{C}_{30}\text{H}_{26}\text{N}_3\text{Cl}_3\text{P}_3\text{Ir}$: C, 47.53; H, 3.46; N, 5.54. Found: C, 47.56; H, 3.50; N, 5.51.

$[\text{IrCl}_3(\text{PPh}_3)(L^b)]$ (**2b**). Yield: 25%, FT-IR (KBr, cm^{-1}): 1595 $[\nu(\text{C}=\text{N})]$, 1380 $[\nu(\text{N}=\text{N})]$, 530, 595 and 750 cm^{-1} $[\nu(\text{PPh}_3)]$, ESI-MS, m/z : 780 $[\text{M}+\text{Na}]^+$. Anal. Calc. for $\text{C}_{30}\text{H}_{26}\text{N}_3\text{Cl}_3\text{P}_3\text{Ir}$: C, 47.53; H, 3.46; N, 5.54. Found: C, 47.57; H, 3.49; N, 5.50. $[\text{IrCl}_3(\text{PPh}_3)(L^c)]$ (**1c**). Yield: 45%, FT-IR (KBr, cm^{-1}): 1615 $[\nu(\text{C}=\text{N})]$, 1405 $[\nu(\text{N}=\text{N})]$, 530, 695 and 745 $[\nu(\text{PPh}_3)]$, ESI-MS, m/z : 801 $[\text{M}+\text{Na}]^+$. Anal. Calc. for

$\text{C}_{29}\text{H}_{23}\text{N}_3\text{Cl}_4\text{P}_3\text{Ir}$: C, 44.74; H, 2.98; N, 5.40. Found: C, 44.77; H, 3.03; N, 5.36.

$[\text{IrCl}_3(\text{PPh}_3)(L^c)]$ (**2c**). Yield: 25%, FT-IR (KBr, cm^{-1}): 1595 $[\nu(\text{C}=\text{N})]$, 1380 $[\nu(\text{N}=\text{N})]$, 530, 595 and 750 cm^{-1} $[\nu(\text{PPh}_3)]$, ESI-MS, m/z : 801 $[\text{M}+\text{Na}]^+$. Anal. Calc. for $\text{C}_{29}\text{H}_{23}\text{N}_3\text{Cl}_4\text{P}_3\text{Ir}$: C, 44.74; H, 2.98; N, 5.40. Found: C, 44.76; H, 3.04; N, 5.42.

4.3.2. Reaction of $[\text{IrCl}_3(\text{PPh}_3)_2]$ with 2-(Arylazo)pyridine (L^{a-c}) in ethanol

4.3.2.1. Isolation of $[\text{IrCl}_3(\text{PPh}_3)(L^a)]$ (2a**), $[\text{IrHCl}_2(\text{PPh}_3)(L^a)]$ (**3a**), $[\text{IrHCl}(\text{PPh}_3)_2(L^a)]\text{Cl}$ (**4a**).** The reaction of $[\text{IrCl}_3(\text{PPh}_3)_2]$ with L^a in 1:1 molar ratio in boiling ethanol produced a greenish brown solution in about 3 h. Three pure compounds of molecular formula $[\text{IrCl}_3(\text{PPh}_3)(L^a)]$ (**2a**), $[\text{IrHCl}_2(\text{PPh}_3)(L^a)]$ (**3a**) and $[\text{IrHCl}(\text{PPh}_3)_2(L^a)]\text{Cl}$ (**4a**) were isolated from the crude mass.

The compounds were purified and isolated from the crude mass on preparative silica-gel TLC plate. The brown compound **3** was eluted first using toluene–chloroform (1:9) solvent mixtures. The other two compounds **2** and **4** moved successively and were eluted with chloroform–acetonitrile (4:1) solvent mixture. The compounds were obtained in different yields depending on the ligands used. Their yields and characterization data are as follows. Notably the sample of **2** obtained from these reactions has exactly identical analytical and spectral properties of the authentic sample of **2** obtained from the reactions described above. $[\text{IrCl}_3(\text{PPh}_3)(L^a)]$ (**2a**). Yield: 10%.

$[\text{IrHCl}_2(\text{PPh}_3)(L^a)]$ (**3a**). Yield: 25%, FT-IR (KBr, cm^{-1}): 1600 $[\nu(\text{C}=\text{N})]$, 1390 $[\nu(\text{N}=\text{N})]$, 535, 695 and 750 $[\nu(\text{PPh}_3)]$, ESI-MS, m/z : 732 $[\text{M}+\text{Na}]^+$. Anal. Calc. for $\text{C}_{29}\text{H}_{25}\text{N}_3\text{Cl}_2\text{P}_3\text{Ir}$: C, 49.08; H, 3.55; N, 5.92. Found: C, 49.11; H, 3.51; N, 5.95.

$[\text{IrHCl}(\text{PPh}_3)_2(L^a)]\text{Cl}$ (**4a**). Yield: 30%, FT-IR (KBr, cm^{-1}): 2140–2185 $[\nu(\text{Ir}-\text{H})]$, 1590 $[\nu(\text{C}=\text{N})]$, 1385 $[\nu(\text{N}=\text{N})]$, 520, 695 and 750 $[\nu(\text{PPh}_3)]$, ESI-MS, m/z : 935 $[\text{M}-\text{Cl}]^+$. Anal. Calc. for $\text{C}_{47}\text{H}_{40}\text{N}_3\text{Cl}_2\text{P}_2\text{Ir}$: C, 58.08; H, 4.15; N 4.32. Found: C, 58.12; H, 4.17; N, 4.35. $[\text{IrCl}_3(\text{PPh}_3)(L^b)]$ (**2b**). Yield: 8%.

$[\text{IrHCl}_2(\text{PPh}_3)(L^b)]$ (**3b**). Yield: 25%, FT-IR (KBr, cm^{-1}): 1600 $[\nu(\text{C}=\text{N})]$, 1390 $[\nu(\text{N}=\text{N})]$, 535, 695 and 750 $[\nu(\text{PPh}_3)]$, ESI-MS, m/z : 746 $[\text{M}+\text{Na}]^+$. Anal. Calc. for $\text{C}_{30}\text{H}_{27}\text{N}_3\text{Cl}_2\text{P}_3\text{Ir}$: C, 49.79; H, 3.76; N, 5.81. Found: C, 49.74; H, 3.80; N, 5.79.

$[\text{IrHCl}(\text{PPh}_3)_2(L^b)]\text{Cl}$ (**4b**). Yield: 30%, FT-IR (KBr, cm^{-1}): 2140–2185 $[\nu(\text{Ir}-\text{H})]$, 1590 $[\nu(\text{C}=\text{N})]$, 1385 $[\nu(\text{N}=\text{N})]$, 520, 695 and 750 $[\nu(\text{PPh}_3)]$, ESI-MS, m/z : 949 $[\text{M}-\text{Cl}]^+$. Anal. Calc. for $\text{C}_{48}\text{H}_{42}\text{N}_3\text{Cl}_2\text{P}_2\text{Ir}$: C, 58.47; H, 4.29; N 4.26. Found: C, 58.45; H, 4.32; N, 4.23. $[\text{IrCl}_3(\text{PPh}_3)(L^c)]$ (**2c**). Yield: 10%.

$[\text{IrHCl}_2(\text{PPh}_3)(L^c)]$ (**3c**). Yield: 25%, FT-IR (KBr, cm^{-1}): 1600 $[\nu(\text{C}=\text{N})]$, 1390 $[\nu(\text{N}=\text{N})]$, 535, 695 and 750 $[\nu(\text{PPh}_3)]$, ESI-MS, m/z : 708 $[\text{M}-\text{Cl}]^+$. Anal. Calc. for $\text{C}_{29}\text{H}_{24}\text{N}_3\text{Cl}_3\text{P}_3\text{Ir}$: C, 46.81; H, 3.25; N, 5.65. Found: C, 46.79; H, 3.28; N, 5.61.

$[\text{IrHCl}(\text{PPh}_3)_2(L^c)]\text{Cl}$ (**4c**). Yield: 30%, FT-IR (KBr, cm^{-1}): 2140–2185 $[\nu(\text{Ir}-\text{H})]$, 1590 $[\nu(\text{C}=\text{N})]$, 1385 $[\nu(\text{N}=\text{N})]$, 520, 695 and 750 $[\nu(\text{PPh}_3)]$, ESI-MS, m/z : 969 $[\text{M}-\text{Cl}]^+$. Anal. Calc. for $\text{C}_{47}\text{H}_{39}\text{N}_3\text{Cl}_3\text{P}_2\text{Ir}$: C, 56.09; H, 3.91; N 4.18. Found: C, 56.12; H, 3.96; N, 4.21.

4.4. Crystallographic measurements

Crystallographic data for the compounds **1c**, **2c**, **3a** and **4c** are collected in Table 1. Suitable X-ray quality crystals of all these are obtained by slow diffusion of a dichloromethane solution of the compound into hexane.

All data were collected on a Bruker SMART APEX-II diffractometer, equipped with graphite monochromated Mo $K\alpha$ radiation ($\lambda = 0.71073 \text{ \AA}$), and were corrected for Lorentz-polarization effects [59,60]. **1c**: A total of 31292 reflections were collected, out of which 8436 are unique ($R_{\text{int}} = 0.0357$) reflections satisfying the $I > 2\sigma(I)$ criterion and were used in subsequent analysis. **2c**: A total of 22989 reflections were collected, out of which 8268 were unique

($R_{\text{int}} = 0.0427$). **3a**: A total of 33928 reflections were collected, out of which 7986 were unique ($R_{\text{int}} = 0.0229$). **4c**: A total of 57261 reflections were collected, out of which 12992 were unique ($R_{\text{int}} = 0.0645$).

All the structures were solved by using SHELXL-97 program package and refined by full-matrix least squares based on F^2 (SHELXL-97) [61,62]. All the hydrogen atoms were added in the calculated positions. Few numbers of diffused scattered peaks were observed in the complex **4c** which can be attributed to disordered solvent molecule. Attempts to model these peaks were unsuccessful because of the diffused nature of the residual electron densities. PLATON/SQUEEZE [63] was used to refine the structure further. A total potential solvent accessible area volume of 129 \AA^3 per unit cell was found.

Acknowledgment

The research was supported by Council of Scientific and Industrial Research, New Delhi (Project, 01/2358/09/EMR-II). Crystallography was performed at the DST-funded National Single Crystal Diffractometer Facility at the Department of Inorganic Chemistry, IACS.

Appendix A. Supplementary material

CCDC 798854–798857 contain the supplementary crystallographic data for this paper. These data can be obtained free of charge from The Cambridge Crystallographic Data Centre via http://www.ccdc.cam.ac.uk/data_request/cif. ^1H NMR spectra, experimental as well as the simulated ESI mass spectra of all the complexes **1–4** are provided as supplementary material. Supplementary data associated with this article can be found, in the online version, at [doi:10.1016/j.ica.2011.02.029](https://doi.org/10.1016/j.ica.2011.02.029).

References

- [1] Z. Huang, J. Zhou, J.F. Hartwig, *J. Am. Chem. Soc.* 132 (2010) 11458.
- [2] T. Ikariya, A.J. Blacker, *Acc. Chem. Res.* 40 (2007) 1300.
- [3] S. Arita, T. Koike, Y. Kayaki, T. Ikariya, *Organometallics* 27 (2008) 2795.
- [4] J.M. McFarland, M.B. Francis, *J. Am. Chem. Soc.* 127 (2005) 13490.
- [5] X. Cui, K. Burgess, *Chem. Rev.* 105 (2005) 3272.
- [6] J.-C. Wasilke, S.J. Obrey, R.T. Baker, G.C. Bazan, *Chem. Rev.* 105 (2005) 1001.
- [7] S. Niu, M.B. Hall, *J. Am. Chem. Soc.* 121 (1999) 3992.
- [8] M.G. Burnett, R.J. Morrison, C.J. Strugnell, *J. Chem. Soc., Dalton Trans.* (1974) 1663.
- [9] G.G. Hlatky, R.H. Crabtree, *Coord. Chem. Rev.* 65 (1985) 1.
- [10] S. Sabo-Etienne, B. Chaudret, *Chem. Rev.* 98 (1998) 2077.
- [11] T. Shima, Y.S. Suzuki, S. Suzuki, *Organometallics* 28 (2009) 871.
- [12] A. Dervisi, C. Carcedo, L. Ooi, *Adv. Synth. Catal.* 348 (2006) 175.
- [13] R.H. Crabtree, *Angew. Chem., Int. Ed. Engl.* 32 (1993) 789.
- [14] G.J. Kubas, *Acc. Chem. Res.* 21 (1988) 120.
- [15] M.A. Garralda, R. Hernández, L. Ibarlucea, E. Pinilla, M.R. Torres, M. Zarrandona, *Organometallics* 26 (2007) 5369.
- [16] M. Panigati, D. Donghi, G. D'Alfonso, P. Mercandelli, A. Sironi, L. D'Alfonso, *Inorg. Chem.* 45 (2006) 10909.
- [17] M. Rosales, T. Gonzalez, R. Atencio, R.A. Sanchez-Delgado, *Dalton Trans.* (2004) 2952.
- [18] D.M. Heinekey, H. Mellows, T. Pratum, *J. Am. Chem. Soc.* 122 (2000) 6498.
- [19] M.A. Esteruelas, M. Olivan, E. Oñate, N. Ruiz, M.A. Tajada, *Organometallics* 18 (1999) 2953.
- [20] W.S. Ng, G. Jia, M.Y. Huang, C.P. Lau, K.Y. Wong, L.B. Wen, *Organometallics* 17 (1998) 4556.
- [21] G. LaMonica, G.A. Ardizzoia, *Prog. Inorg. Chem.* 46 (1997) 151.
- [22] A.P. Sadimenko, S.S. Bassoon, *Coord. Chem. Rev.* 147 (1996) 247.
- [23] S. Trofimenko, *Prog. Inorg. Chem.* 34 (1986) 115.
- [24] S. Trofimenko, *Chem. Rev.* 72 (1972) 497.
- [25] G. Albertin, S. Antoniutti, J. Castro, S. Garcia-Fontán, E. Gurabardhi, *J. Organomet. Chem.* 691 (2006) 1012.
- [26] R. Peloso, R. Pattacini, C.S.J. Cazin, P. Braunstein, *Inorg. Chem.* 48 (2009) 11415.
- [27] M. Jiménez-Tenorio, M.C. Puerta, P. Valerga, *Organometallics* 28 (2009) 2787.
- [28] C. Tejel, M.A. Ciriano, M. Millaruelo, J.A. Lopez, F.J. Lahoz, L.A. Oro, *Inorg. Chem.* 42 (2003) 4750.
- [29] N. Paul, S. Samanta, S. Goswami, *Inorg. Chem.* 49 (2010) 2649.
- [30] A. Sanyal, P. Banerjee, G.-H. Lee, S.-M. Peng, C.-H. Hung, S. Goswami, *Inorg. Chem.* 43 (2004) 7456.
- [31] S. Samanta, P. Singh, J. Fiedler, S. Zălis, W. Kaim, S. Goswami, *Inorg. Chem.* 47 (2008) 1625.
- [32] M. Panda, C. Das, G.-H. Lee, S.-M. Peng, S. Goswami, *Dalton Trans.* (2004) 2655.
- [33] M. Sinan, M. Panda, P. Banerjee, C.B. Shinisha, R.B. Sunoj, S. Goswami, *Org. Lett.* 11 (2009) 3218.
- [34] S. Mandal, N. Paul, P. Banerjee, T.K. Mondal, S. Goswami, *Dalton Trans.* 39 (2010) 2717.
- [35] S. Joy, P. Pal, M. Mahato, G.B. Talapatra, S. Goswami, *Dalton Trans.* 39 (2010) 2775.
- [36] M. Sinan, M. Panda, A. Ghosh, K. Dhara, P.E. Fanwick, D.J. Chattopadhyay, S. Goswami, *J. Am. Chem. Soc.* 130 (2008) 5158.
- [37] G.C. Bond, *Platinum Met. Rev.* 44 (2000) 146.
- [38] C.F.J. Barnard, W. Weston, *Platinum Met. Rev.* 43 (1999) 158.
- [39] N. Paul, T. Krämer, J.E. McGrady, S. Goswami, *Chem. Commun.* 46 (2010) 7124.
- [40] A.R. McDonald, M. Lutz, L.S. von Chrzanowski, G.P.M. van Klink, A.L. Spek, G. van Koten, *Inorg. Chem.* 47 (2008) 6681, and references therein.
- [41] K.Y. Zhang, K.K. Lo, *Inorg. Chem.* 48 (2009) 6011.
- [42] K.L. Haas, K.J. Franz, *Chem. Rev.* 109 (2009) 4921.
- [43] M. Yu, Q. Zhao, L. Shi, F. Li, J. Zhou, H. Wang, T. Yi, C. Huang, *Chem. Commun.* 18 (2008) 2115.
- [44] D.-L. Ma, W.-L. Wong, W.-H. Chung, F.-Y. Chan, P.-K. So, T.-L. Lai, Z.-Y. Zhou, Y.-C. Leung, K.-Y. Wong, *Angew. Chem. Int. Ed.* 47 (2008) 3735, and references therein.
- [45] M.A. Bennett, D.L. Milner, *J. Am. Chem. Soc.* 91 (1969) 6983.
- [46] L. Vaska, J.W. Diluzio, *J. Am. Chem. Soc.* 83 (1961) 2784.
- [47] L. Vaska, *J. Am. Chem. Soc.* 83 (1961) 756.
- [48] S. Basu, I. Pal, R.J. Butcher, G. Rosair, S. Bhattacharya, *J. Chem. Sci.* (2005) 167.
- [49] R. Acharyya, F. Basuli, R.-Z. Wang, T.C.W. Mak, S. Bhattacharya, *Inorg. Chem.* 43 (2004) 704.
- [50] T. Dirnberger, H. Werner, *Organometallics* 24 (2005) 5127, and references therein.
- [51] R.P. Hughes, I. Kovacic, D.C. Lindner, J.M. Smith, S. Willemsen, D. Zhang, I.A. Guzei, L. Rheingold, *Organometallics* 20 (2001) 3190, and references therein.
- [52] W. Clegg, A.J. Scott, N.C. Norman, E.G. Robins, G.R. Whittell, *Acta Crystallog., Section E: Structure Reports Online* E58 (2002) m408.
- [53] M.A. Bennett, S.K. Bhargava, M. Ke, A.C. Willis, *J. Chem. Soc., Dalton Trans.* (2000) 3537.
- [54] K.D. Schramm, J.A. Ibers, *Inorg. Chem.* 19 (1980) 1231.
- [55] A. Saha, C. Das, S. Goswami, S.-M. Peng, *Ind. J. Chem. Sec. A* 40A (2001) 198.
- [56] K.K.-W. Lo, C.-K. Chung, N. Zhu, *Chem. Eur. J.* 9 (2003) 475.
- [57] D.T. Sawyer, J.L. Roberts Jr., *Experimental Electrochemistry for Chemists*, John Wiley and Sons, NY, 1974.
- [58] N. Campbell, A.W. Henderson, D.J. Taylor, *J. Chem. Soc.* (1953) 1281.
- [59] Bruker SMART and SAINT. Area Detector Control and Integration Software, Bruker Analytical X-ray Instruments Inc.; Madison, Wisconsin, USA, 1997.
- [60] G.M. Sheldrick, SADABS, Program for Empirical Absorption Correction of Area Detector Data, University of Göttingen, Germany, 1997.
- [61] G.M. Sheldrick, *Acta Cryst.* A46 (1990) 467.
- [62] G.M. Sheldrick, SHELXL-97, Program for the refinement of crystal structures, University of Göttingen, Göttingen, Germany, 1997.
- [63] A.L. Spek, *J. Appl. Crystallogr.* 36 (2003) 7.